

# Homogeneous Hypersurface Spacetime with Topological Defects in $f(G)$ Gravity

S.P. Hatkar<sup>1</sup>, P.A. Agre<sup>2</sup>, D.P. Tadas<sup>3</sup>, R.T. Idhole<sup>1</sup>,  
S.D. Katore<sup>4</sup>

<sup>1</sup>Department of Mathematics, A.E.S. Arts, Commerce and Science College, Hingoli-431513, India

<sup>2</sup>Department of Mathematics, K.J. Somaiya College of Science and Commerce, Mumbai, India

<sup>3</sup>Department of Mathematics, Toshniwal Arts, Commerce and Science College, Sengaon-431542, India

<sup>4</sup>Department of Mathematics, Sant Gadge Baba Amravati University Amravati-444602, India

Received 24 March 2026

**Abstract.** In this Paper, we have studied hypersurface homogeneous space time in the presence of cosmic string and domain walls in the context of  $f(G)$  theory of gravitation. Field equations are solved by using generalized linearly varying deceleration parameter. Some physical parameters are also investigated.

KEY WORDS: Homogeneous hypersurface space time, Cosmic String, Domain Walls,  $f(G)$  gravity.

## 1 Introduction

After successful proposal of General Theory of relativity by Einstein in 1915 [1], it found that general theory of relativity faces various unresolved issues when applied to the broader concept of cosmology [2]. Additionally, the theory predicts singularities such as those at the centre of black holes and at the big bang, where physical laws break down and quantities become infinite. These problems forced to formulate modified theories  $f(R)$ ,  $f(T)$ ,  $f(G)$ ,  $f(R, T)$ ,  $f(R, L_m)$  theories which motivate to work on issues in cosmology [3–7]. Among the several modifications of general theory of relativity,  $f(G)$  theory of gravitation has potential to address fundamental issues in cosmology. Firstly, proposed by Nojiri and Odintsov [8] by adding terms of Gauss Bonnet function of  $f(G)$  to the Hilbert action which helps to explain higher order curvature corrections that provides geometric structure of space time. Motivation behind to study  $f(G)$  theory has capacity to explain the accelerated expansion of the universe without raising dark energy in its standard form [9]. Moreover, it produces a unified framework that can account for both the early-time inflationary period and

late time cosmic acceleration [3]. These things make  $f(G)$  gravity a promising candidate for knowing the complete dynamical history of the universe and for addressing challenges that remain unresolved within the framework of general relativity theory.

In this context, Cognola et al. [3] proposed a feasible model by extending the Einstein-Hilbert action with such a function, showing that it can effectively account for cosmic acceleration associated with dark energy and offers a potential resolution to the hierarchy problem. Marcos et al. [10] discussed the solution of regular black holes from general relativity to  $f(G)$  gravity and it arise due to coupling between gravitational theory and nonlinear electrodynamics. Yousaf et al. [11] investigated the effect of certain physical parameters on pressure anisotropy in dynamic, spherically symmetric stellar systems within the context of Gauss Bonnet modified gravity, with importance on the role of the weyl scalar in the evolution of stellar structures. Abbas at el. [12] examine the potential formation of anisotropic compact stars within the framework of  $f(G)$  gravity, a modified Gauss–Bonnet theory proposed to describe the accelerated expansion of the universe. Recent research explore the cosmological and astrophysical consistency of  $f(G)$  gravity models through the implementation of conditions on stable late-time de Sitter solutions, consistent evolution during radiation, matter, and accelerated eras, and solar system constraint agreement; taking into account flat space time and perfect fluid models, certain types of  $f(G)$  are explore for singularity resolution of finite-time future singularities, with model parameters bounded by observational measurements like the Hubble constant, deceleration, jerk, and snap, and tested using classical tests such as deflection of light and precession of perihelion [13–15].

Topological defects arise during symmetry breaking phase transition in the very early universe. Based on the vacuum manifold's topology and the associated homotopy groups, these defects which include domain walls, cosmic strings, monopoles and textures are categorized. Topological defects play important role in structure formation and galaxy formation because it carries energy and it leads to an extract attractive gravitation force and therefore defects acts as seeds for cosmic structures [16–18]. Domain walls, which occur when a discrete symmetry is spontaneously broken, are especially important in models involving scalar fields, where their dynamics can shape large-scale structure and effect the thermal history of the universe. Skenderis et al. [19] studied the significant of domain walls configuration in four dimensional supergravity, explained how they connect supersymmetric AdS vacua and pseudo supersymmetric AdS cosmologies via twisted spinor structures. Abel at al. [19] investigated the cosmological effect of the supersymmetric Standard Model extended with a gauge singlet, emphasizing the evolution of domain walls resulting from the discrete  $Z_3$  symmetry during electroweak symmetry breaking as a potential solution to the  $\mu$ -problem.

The above discussions motivated us to investigate the behaviour of topological defects within the framework of  $f(G)$  theory of gravity. In this paper, we in-

investigate the exact solutions of a homogeneous hypersurface spacetime in the presence of topological defects. We investigate two different forms of the deceleration parameter  $q$ . The solution of the  $f(G)$  gravity field equations obtained using  $q = -b(t) - 1$  and  $q = -1 + l/(1 + a^l)$  are presented in Section 3 and Section 4, respectively. We also discussed the behaviour of several cosmological parameters, such as the jerk, snap, and mean anisotropy parameter, which gives more detailed information on the dynamical evolution of the universe under this modified gravity model. Finally, in Section 5 we conclude our findings.

## 2 The Basic of $f(G)$ Gravity and Metric Formalism

The action of  $f(G)$  theory of gravity corresponding to the matter Lagrangian  $S_\phi$  [9] as

$$S_1 = \frac{1}{2L} \int [R + f(G)] \sqrt{-g} d^4x + S_\phi(g^{ij}, \phi), \quad (1)$$

where  $g$  is the determinant of the metric tensor  $g_{ij}$ ,  $L^2 = 8\pi G_n$ ,  $G_n$  is the constant of Newtonian,  $S_\phi$  is the action of matter,  $R$  is a Ricci scalar. The matter is minimally coupled to the metric tensor  $g_{ij}$  which means  $f(G)$  is an arbitrary function of Gauss-Bonnet invariant  $G$  which is given by

$$G = R^2 - 4R_{ij}R^{ij} + R_{ij\mu\nu}R^{ij\mu\nu}, \quad (2)$$

where  $R_{ij}$  stands for Ricci tensor and  $R_{ij\mu\nu}$  denotes Riemannian tensors. We obtain the field equation by varying the action (1) with respect to the metric  $g_{ij}$  as

$$R_{ij} - \frac{1}{2}Rg_{ij} + \delta \left\{ R_{i\mu j\nu} + R_{\mu j g_{\nu i}} - R_{\mu\nu}g_{ji} - R_{ij}g_{\nu\mu} + R_{i\nu}g_{j\mu} \right. \\ \left. + \frac{1}{2}R(R_{ij}g_{\mu\nu} - g_{i\nu}g_{j\mu}) \right\} \nabla^\mu \nabla^\nu + (Gf_G - f)g_{ij} = LT_{ij}, \quad (3)$$

here  $\nabla_\mu$  denotes the covariant derivative and  $f_G \equiv \frac{df}{dG}$ . Homogeneous hypersurface play a crucial role in cosmology by enabling the simplification of complex gravitational dynamics through symmetry assumptions. Their spatial uniformity allows one to express the gravitational field equations in a reduced form, making the analysis of large-scale cosmic behavior more tractable [20]. Recently, Gielen et al. [21] emphasized the utility of homogeneous hypersurface in cosmology for simplifying the dynamics of the universe and formulating initial conditions in quantum gravity frameworks. Similarly, Ashtekar et al. [22] has highlighted their importance in the Hamiltonian formulation of general relativity, particularly in the context of loop quantum cosmology. so we consider the Homogeneous Hyper surface space time in the form

$$ds^2 = -dt^2 + A^2 dx^2 + B^2 (dy^2 + S^2(y, k) dz^2), \quad (4)$$

#### 4 Homogeneous Hypersurface Spacetime with Topological Defects in...

where  $A, B$  are functions of  $t$  and  $S(y, k) = \sinh y, y, \sin y$  respectively when  $k = -1, 0, 1$ .

The Ricci tensor and Gauss-Bonnet invariant are obtained as

$$R = 2 \left[ \frac{A_{44}}{A} + \frac{2A_4 B_4}{AB} + \frac{2B_{44}}{B} + \frac{k}{B^2} \right] \quad (5)$$

$$G = \frac{8A_{44}B_4^2}{AB^2} + \frac{8kA_{44}}{AB^2} + \frac{16A_4 B_4 B_{44}}{AB^2}, \quad (6)$$

where ‘4’ here and elsewhere denotes differential with respect to  $t$ .

The energy momentum tensor  $T_{\mu\nu}$  of Cosmic string and domain walls is given as

$$T_{\mu\nu} = \rho_{\text{eff}} (g_{\mu\nu} + p_d u_\mu u_\nu - \lambda x_\mu x_\nu) \quad (7)$$

with  $u_\mu u^\nu = x_\mu x^\nu = -1$ ,  $\rho_{\text{eff}} = \rho_d + \lambda$  is the effective energy density of domain walls and cosmic string.  $\rho_d$  stands for energy density of domain wall,  $p_{\text{eff}}$  represents the pressure and  $\lambda$  denotes the string of  $x$ -axis.  $u_\mu$  is the component of the four velocity vector, and  $x^\mu$  is the direction of the string.

Now the domain wall consist of normal matter  $\rho_m$  pressure  $p_m$  and tension  $\sigma_d$ , and they are related in the following way  $p_d = p_m - \sigma_d$  and  $\rho_d = \rho_m + \sigma_d$

Using equation (4) and (7) field equations are obtained as

$$\begin{aligned} \frac{-2B_{44}}{B} - \frac{B_4^2}{B^2} - \frac{k}{B^2} - \frac{16B_4 B_{44}}{B^2} \dot{f}_G - 8 \left\{ \frac{B_4^2}{B^2} + \frac{k}{B^2} \right\} \ddot{f}_G \\ + G \dot{f}_G - f = \rho_{\text{eff}} + \lambda, \end{aligned} \quad (8)$$

$$\begin{aligned} \frac{A_{44}}{A} - \frac{A_4 B_4}{AB} - \frac{B_{44}}{B} - 8 \left\{ \frac{A_4 B_{44} + B_4 A_{44}}{AB} \right\} \dot{f}_G - \frac{8A_4 B_4}{AB} \ddot{f}_G \\ + G \dot{f}_G - f = \rho_{\text{eff}}, \end{aligned} \quad (9)$$

$$\begin{aligned} \frac{-2A_4 B_4}{AB} - \frac{B_4^2}{B^2} - \frac{k}{B^2} - \left\{ \frac{24A_4 B_4^2 + 8kA_4}{AB^2} \right\} \dot{f}_G \\ + G \dot{f}_G - f = -p_d. \end{aligned} \quad (10)$$

Clearly, we have system of three equations (8) to (10) in six unknown  $A, B, \rho_{\text{eff}}, \lambda, p_d$  and  $f$ . To obtain the solution of the system completely, we need three more conditions:

- Initially, we assume shear scalar  $\sigma$  is proportional to expansion scalar  $\theta$  leads to the relation

$$A = B^n, \quad (11)$$

where  $n$  is arbitrary. The condition  $A = B^n$  imposes a relation between metric functions that reduces the complexity of anisotropic cosmological models, allowing the field equations to be more tractable and solvable [23].

- Secondly, we choose the functional form of  $f(G)$  in Gauss-Bonnet gravity introduces specific curvature corrections that facilitate obtaining exact cosmological solutions with desired physical properties [24] as the

$$f(G) = \alpha G^{\beta+1}, \quad (12)$$

where,  $\alpha$  and  $\beta$  are model parameters.

- Lastly, we consider two different generalized forms of linearly varying deceleration parameter as  $q = -a\ddot{a}/\dot{a}^2 = -b(t) - 1$  and  $q = -1 + l/(1 + a^l)$ , where  $l > 0$  is constant. Together, these assumptions enable the exploration of rich cosmological behaviour within modified gravity frameworks while keeping the equations analytically manageable.

### 3 Case-I

In this case, we consider the generalized form of linearly varying deceleration parameter as

$$q = -\frac{a\ddot{a}}{\dot{a}^2} = -b(t) - 1. \quad (13)$$

We assume the function  $b(t)$  in following form:

$$b(t) = -\sec h^2 t. \quad (14)$$

Therefore, the deceleration parameter  $q$  and scale factor  $a$  are found to be

$$q = \sec h^2 t - 1, \quad (15)$$

$$a(t) = \sinh(t). \quad (16)$$

The sign of the deceleration parameter  $q$  tells one whether the universe is decelerating or accelerating. Positive sign indicates decelerating universe while negative sign represent accelerating universe. Clearly from Figure 1, it is observed that, the universe is accelerating at the present. Using (11), (13) and (16), we get the values of metric potentials  $A$  and  $B$  as

$$A = (\sinh t)^{\frac{3n}{n+2}} \quad \text{and} \quad B = (\sinh t)^{\frac{3}{n+2}} \quad (17)$$

The Cosmological parameters such as the Hubble parameter  $H$  characterizes the rate of the expansion of the universe as a function of cosmic time. Hubble parameter  $H$  is obtained as  $H = \dot{a}/a = \coth t$ , expansion scalar  $\theta$  and shear scalar  $\sigma$  are obtained as

$$\theta = \frac{A_4}{A} + \frac{2B_4}{B} = 3 \coth t, \quad (18)$$

$$\sigma = \frac{1}{\sqrt{3}} \left( \frac{A_4}{A} - \frac{B_4}{B} \right) = \frac{\sqrt{3}(n-1)}{(n+2)} \coth t \quad (19)$$

6 Homogeneous Hypersurface Spacetime with Topological Defects in...

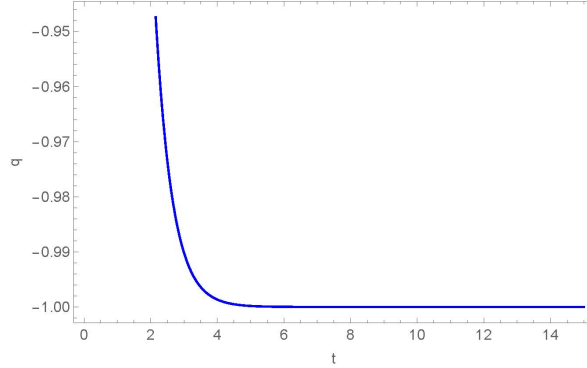


Figure 1. Graph of deceleration parameter  $q$  vs. time  $t$

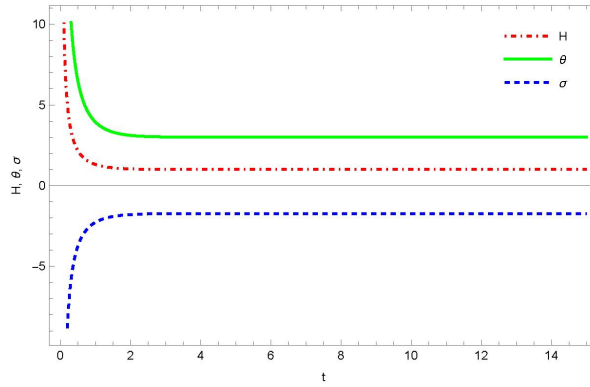


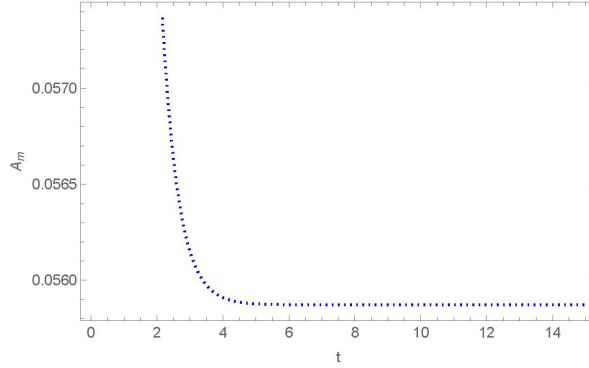
Figure 2. Graph of  $H$ ,  $\theta$  and  $\sigma$  vs. time  $t$

The mean anisotropic parameter  $A_m$  measures deviations from isotropic expansion in the universe [25]. It is obtained as

$$A_m = \frac{2}{9H^2} \left( \frac{A_4}{A} - \frac{B_4}{B} \right)^2 = \frac{2(n-1)^2}{(n+2)^2}. \quad (20)$$

From Figure 3, the mean anisotropic parameter  $A_m$  is a positive decreasing function of cosmic time  $t$ . It indicates an initially anisotropic universe evolving toward isotropy, consistent with current cosmological observations. The Gauss-Bonnet invariant  $G$  is obtained as

$$G = m_{15} \coth^4 t + 27m_3 \tanh^2 t + 48knm_4 \sinh^{-2m_{11}} t \cosh^2 t + 24km_7 \sinh^{-6m_{12}} t. \quad (21)$$

Figure 3. Graph of mean anisotropic parameter  $A_m$  vs. time  $t$ .

On solving equations (8), (9) and (10) using above conditions, we get

$$\begin{aligned}
\rho_{\text{eff}} = & -3m_1 \sinh^{-2} t + 9m_2 - 24m_3 \coth t (3(1-n) \sinh^{-2} t + 9) \\
& \times \alpha(\beta+1)\beta G^{\beta-1} \left\{ -5184m_7^2 \coth^3 t \csc h^2 t + 54m_3 \tanh t \text{sech}^{2t} \right. \\
& \left. - 96m_5 \sinh^{-3m_8}(t) + m_{17} \sinh^{-m_9}(t) \right\} \\
& - 72m_7 \sinh^{-2} t \cosh^2 t \left[ \alpha(\beta+1)\beta(\beta-1) \text{csch}^2 t G^{\beta-2} \right. \\
& \times \left\{ -5184m_7^2 \coth^3 t \text{csch}^2 t + 54m_3 \tanh t \text{sech}^2 t \right. \\
& \left. - 96m_5 \sinh^{-3m_8}(t) + m_{17} \sinh^{-m_9}(t) \right\}^2 + \alpha(\beta+1)\beta G^{\beta-1} \\
& \times \left\{ -5184m_7^2 (-5 \coth^{2t} + 3) \coth^{2t} \text{csch}^2 t \right. \\
& + 54m_3 (1 - 3 \tanh^2 t) \text{sech}^2 t + 288m_5 m_8 \sinh^{-2m_{10}}(t) \cosh t \\
& \left. \left. + m_{16} \sinh^{-2m_{11}}(t) \cosh t + 16m_6 \sinh^{-6m_{12}}(t) \right\} \right] + \alpha\beta G^{\beta+1}. \quad (22)
\end{aligned}$$

Clearly from Figures 4(a), 5(a) and 6(a) for  $k = 1$ ,  $k = 0$  and  $k = -1$ , the effective density  $\rho_{\text{eff}}$  is decreases as time  $t$  increases. it is approaches to zero as time  $t \rightarrow \infty$ . for  $k = 0$ .

From Eqs. (8), (9), (11), (16) and (17), we get string tension density  $\lambda$ . From Figure 4(b) for  $k = 1$ , the string tension density  $\lambda$  is a decreasing function of time  $t$ . It approaches to zero as time  $t \rightarrow \infty$ . Figures 5(b) and 6(b) show the string density  $\lambda$  is negative increasing function of time  $t$  and  $\lambda \rightarrow 0$  as time  $t \rightarrow \infty$  [26].

8 Homogeneous Hypersurface Spacetime with Topological Defects in...

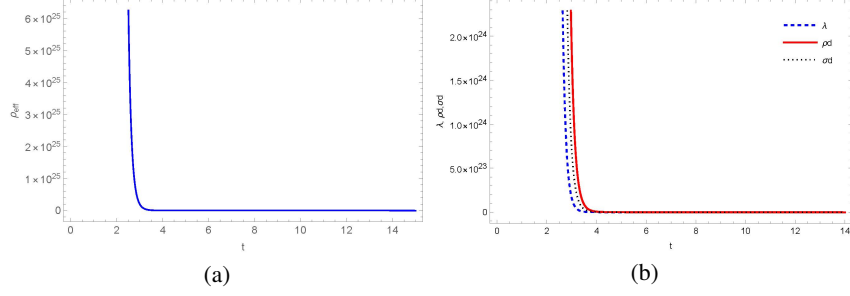


Figure 4. Graph of  $\rho_{\text{eff}}$ ,  $\lambda$ ,  $\rho_d$ ,  $\sigma_d$  vs. time  $t$  for  $k = 1$ ,  $\alpha = -3$ ,  $\beta = 20$ ,  $n = 11.5$ .

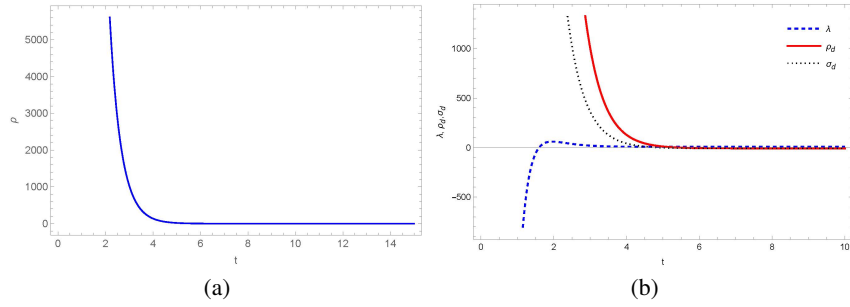
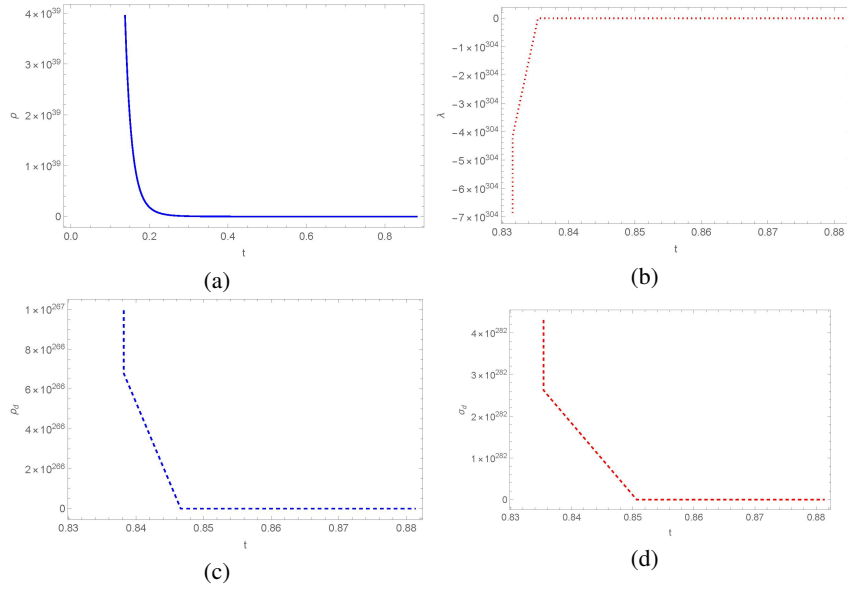


Figure 5. Graph of  $\rho_{\text{eff}}$ ,  $\lambda$ ,  $\rho_d$ ,  $\sigma_d$ , vs. time  $t$  for  $k = 0$ ,  $\alpha = 6.5$ ,  $\beta = -0.6$ ,  $n = 14$ .

$$\begin{aligned}
 \lambda = & (m_{18} + 9m_4 \cosh^2 t) \sinh^{-2} t + 9m_{13} - k \sinh^{-6m_{12}} t - \alpha(\beta + 1)\beta G^{\beta-1} \\
 & \times \left[ 144m_4 m_{12} \sinh^{-3m_{19}} t \cosh t - 432m_{12}^3 \sinh^{m_{20}} t \cosh t \right. \\
 & \left. + 72m_4 m_7 \sinh^{-3} t \cosh t + 216m_7 m_{14} \sinh^{-1} t \cosh t \right] \\
 & \times \left\{ 5184m_7^2 \coth^3 t^2 t - 54m_3 \tanh t^2 t + 96m_5 \sinh^{-3m_8}(t) \right. \\
 & \left. - m_{17} \sinh^{-m_9}(t) \right\} + 8 \left[ 9m_4 \sinh^{-2} \cosh^2 t - k \sinh^{-6m_{12}} \right] \\
 & \times \left[ \alpha(\beta + 1)\beta(\beta - 1)G^{\beta-2} + \left\{ -5184m_7^2 \coth^3 t \operatorname{csch}^2 t \right. \right. \\
 & \left. \left. + 54m_3 \tanh t \operatorname{sech}^2 t - 96m_5 \sinh^{-3m_8}(t) + m_{17} \sinh^{-m_9}(t) \right\}^2 \right. \\
 & \left. + \alpha(\beta + 1)\beta G^{\beta-1} \left\{ -5184m_7^2(-5 \coth^2 t + 3) \coth^2 t \operatorname{csch}^2 t \right. \right. \\
 & \left. \left. + 54m_3(1 - 3 \tanh^2 t) \operatorname{sech}^2 t + 288m_5 m_8 \sinh^{-2m_{10}}(t) \cosh t \right. \right. \\
 & \left. \left. + m_{16} \sinh^{-2m_{11}}(t) \cos ht + 16m_6 \sinh^{-6m_{12}}(t) \right\} \right]. \quad (23)
 \end{aligned}$$

Figure 6. Graph of  $\rho_{\text{eff}}$ ,  $\lambda$ ,  $\rho_d$ ,  $\sigma_d$  vs. time  $t$ ,  $k = -1$ ,  $\alpha = 0.2$ ,  $\beta = 1.1$ ,  $n = -2.001$ .

After solving equations (10), (11), (16) and (17), the pressure of fluid is obtained

$$\begin{aligned}
 P_d = & 9m_{21} \sinh^{-2} t \cosh^2 t + k \sinh^{-6m_{12}}(t) + \alpha(\beta + 1)\beta G^{\beta-1} \\
 & \times \left[ 648m_3 \sinh^{-3} t \cosh^3 t + 24km_7 \sinh^{-m_9} t \cosh t \right] \\
 & \times \left\{ -5184m_7^2 \coth^3 t \operatorname{csch}^2 t + 54m_3 \tanh t \operatorname{sech}^2 t \right. \\
 & \left. - 96m_5 \sinh^{-3m_8}(t) + m_{17} \sinh^{-m_9}(t) \right\} - \alpha\beta G^{\beta+1}, \quad (24)
 \end{aligned}$$

where

$$\begin{aligned}
 m_1 &= \frac{2n^2 + 2n - 1}{(n+2)^2}, \quad m_2 = \frac{n^2 - n - 1}{(n+2)^2}, \quad m_3 = \frac{n}{(n+2)^3}, \\
 m_4 &= \frac{n-1}{(n+2)^2}, \quad m_5 = \frac{kn(n-1)(n+5)}{(n+2)^3}, \quad m_6 = \frac{kn(6n-15)}{(n+2)^2}, \\
 m_7 &= \frac{n}{n+2}, \quad m_8 = \frac{n+4}{n+2}, \quad m_9 = \frac{n+8}{n+2}, \quad m_{10} = \frac{2n+7}{n+2}, \\
 m_{11} &= \frac{n+5}{n+2}, \quad m_{12} = \frac{1}{n+2}, \quad m_{13} = \frac{n^2-1}{(n+2)^2}, \quad m_{14} = \frac{n+1}{(n+2)^2}, \\
 m_{15} &= 1296m_3m_7, \quad m_{16} = (96m_5m_9 - 16m_9m_6), \\
 m_{17} &= (-96m_5 + 16m_6 \cosh t), \quad m_{18} = 3(m_7^2 + m_2), \quad m_{19} = (2m_7 + m_{12}),
 \end{aligned}$$

10 *Homogeneous Hypersurface Spacetime with Topological Defects in...*

$$m_{20} = m_{12} - 4m_7, \quad m_{21} = (2m_{12}m_7 + m_{12}^2),$$

$$m_{22} = [9m_4 - 9(2m_7m_{12} + m_{12}^2)], \quad m_{23} = 3m_1 + m_{18}.$$

Now using equations (22) and (23), the energy density of the domain wall is obtained as

$$\begin{aligned} \rho_d = & - \left\{ m_{23} + 9m_4 \cosh^2 t \right\} \sinh^{-2} t - 9m_{13} + k \sinh^{-6m_{12}}(t) \\ & + \left[ 24m_3 \coth t (3(1-n) \sinh^{-2} t + 9) + 144m_4m_{12} \sinh^{-3m_{19}}(t) \cosh t \right. \\ & - 432m_{12}^3 \sinh^{m_{20}}(t) \cosh t + 72m_4m_7 \sinh^{-3} t \cosh t \\ & \left. + 216m_7m_{14} \sinh^{-1} t \cosh t \right] \alpha(\beta+1)\beta G^{\beta-1} \left\{ 5184m_7^2 \coth^3 t \csc h^2 t \right. \\ & \left. - 54m_3 \tanh t \sec h^2 t + 96m_5 \sinh^{-3m_8}(t) - m_{17} \sinh^{-m_9}(t) \right\} \\ & - \left[ 72(m_7 + m_4) \sinh^{-2} t \cosh^2 t - 8k \sinh^{-6m_{12}}(t) \right] \\ & \times \left[ \alpha(\beta+1)\beta(\beta-1)G^{\beta-2} \left\{ -5184m_7^2 \coth^3 t \csc h^2 t \right. \right. \\ & \left. \left. + 54m_3 \tanh t \operatorname{sech}^2 t - 96m_5 \sinh^{-3m_8}(t) + m_{17} \sinh^{-m_9}(t) \right\}^2 \right. \\ & \left. + \alpha(\beta+1)\beta G^{\beta-1} \left\{ -5184m_7^2(-5 \coth^2 t + 3) \coth^2 t \operatorname{csch}^2 t \right. \right. \\ & \left. \left. + 54m_3(1-3 \tanh^2 t) \operatorname{sech}^2 t + 288m_5m_8 \sinh^{-2m_{10}}(t) \cosh t \right. \right. \\ & \left. \left. + m_{16} \sinh^{-2m_{11}}(t) \cosh t + 16m_6 \sinh^{-6m_{12}}(t) \right\} \right] + \alpha\beta G^{\beta+1}. \quad (25) \end{aligned}$$

From Figures 4(b), 5(b) and 6(c), the energy density  $\rho_d$  of domain wall is positive and decreasing function of time  $t$ . It approaches to zero as time  $t$  increases. On solving equation (24) and (25), we get the normal matter of domain wall

$$\begin{aligned} \gamma\rho_m = & -(m_{23} + m_{22} \cosh^2 t) \sinh^{-2} t - 9m_{13} + k \sinh^{-6m_{12}}(t) \\ & - \left[ 72(9m_3 \cosh^3 t - m_4m_7) \sinh^{-3} t \cosh t \right. \\ & + 24km_7 \sinh^{-m_9} t \cosh t - 24m_3(3(1-n) \sinh^{-2} t + 9) \coth t \\ & + 144m_4m_{12} \sinh^{-3(2m_7+m_{12})}(t) \cosh t + 432m_{12}^3 \sinh^{m_{20}}(t) \cosh t \\ & \left. + 216m_7m_{14} \sinh^{-1} t \cosh t \right] \alpha(\beta+1)\beta G^{\beta-1} \left\{ -5184m_7^2 \coth^3 t \operatorname{csch}^2 t \right. \\ & \left. + 54m_3 \tanh t \sec h^2 t - 96m_5 \sinh^{-3m_8}(t) + m_{17} \sinh^{-m_9}(t) \right\} \\ & - \left[ 72(m_7 + m_4) \sinh^{-2} t \cosh^2 t - 8k \sinh^{-6m_{12}}(t) \right] \end{aligned}$$

$$\begin{aligned}
& \times \left[ \alpha(\beta + 1)\beta(\beta - 1)G^{\beta-2} \left\{ -5184m_7^2 \coth^3 t \operatorname{csch}^2 t \right. \right. \\
& \left. \left. + 54m_3 \tanh t \sec^2 t - 96m_5 \sinh^{-3m_8}(t) + m_{17} \sinh^{-m_9}(t) \right\}^2 \right. \\
& \left. + \alpha(\beta + 1)\beta G^{\beta-1} \left\{ -5184m_7^2(-5 \coth^2 t + 3) \coth^2 t \operatorname{csch}^2 t \right. \right. \\
& \left. \left. + 54m_3(1 - 3 \tanh^2 t) \operatorname{sech}^2 t + 288m_5 m_8 \sinh^{-2m_{10}}(t) \cosh t \right. \right. \\
& \left. \left. + m_{16} \sinh^{-2m_{11}}(t) \cosh t + 16m_6 \sinh^{-6m_{12}}(t) \right\} \right]. \quad (26)
\end{aligned}$$

On solving equations (25) and (26), we get the tension  $\sigma_d$  of domain wall

$$\begin{aligned}
\sigma_d = & - \left[ (m_{23} + 9m_4 \cosh^2 t) \left(1 - \frac{1}{\gamma}\right) + \frac{9}{\gamma} m_{21} \cosh^2 t \right] \sinh^{-2} t \\
& - \left(1 - \frac{1}{\gamma}\right) 9m_{13} + \left(1 - \frac{2}{\gamma}\right) k \sinh^{-6m_{12}}(t) \\
& + \left[ 24m_3 \coth t (3(1 - n) \sinh^{-2} t + 9) \left(1 - \frac{1}{\gamma}\right) \right. \\
& \left. + 144m_4 m_{12} \sinh^{-3m_{19}}(t) \cosh t \left(1 - \frac{1}{\gamma}\right) - 432m_{12}^3 \sinh^{m_{20}} t \right. \\
& \left. \times \cosh t \left(1 - \frac{1}{\gamma}\right) + 72 \left(\frac{9}{\gamma} m_3 \cosh^2 t + \left(1 - \frac{1}{\gamma}\right) m_4 m_7\right) \sinh^{-3} t \cosh t \right. \\
& \left. + 216m_7 m_{14} \left(1 - \frac{1}{\gamma}\right) \sinh^{-1} t \cosh t + \frac{24}{\gamma} k m_7 \sinh^{-m_9} t \cosh t \right] \\
& \times \alpha(\beta + 1)\beta G^{\beta-1} \left\{ 5184m_7^2 \coth^3 t \operatorname{csch}^2 t - 54m_3 \tanh t \operatorname{sech}^2 t \right. \\
& \left. + 96m_5 \sinh^{-3m_8} t - m_{17} \sinh^{-m_9}(t) \right\} \\
& - \left(1 - \frac{1}{\gamma}\right) \left[ 72(m_7 + m_4) \sinh^{-2} t \cosh^2 t - 8k \sinh^{-6m_{12}}(t) \right] \\
& \times \left[ \alpha(\beta + 1)\beta(\beta - 1)G^{\beta-2} \left\{ -5184m_7^2 \coth^3 t \operatorname{csch}^2 t \right. \right. \\
& \left. \left. + 54m_3 \tanh t \operatorname{sech}^2 t - 96m_5 \sinh^{-3m_8}(t) + m_{17} \sinh^{-m_9}(t) \right\}^2 \right. \\
& \left. + \alpha(\beta + 1)\beta G^{\beta-1} \left\{ -5184m_7^2(-5 \coth^2 t + 3) \coth^2 t \operatorname{csch}^2 t \right. \right. \\
& \left. \left. + 54m_3(1 - 3 \tanh^2 t) \operatorname{sech}^2 t + 288m_5 m_8 \sinh^{-2m_{10}}(t) \cosh t \right. \right. \\
& \left. \left. + m_{16} \sinh^{-2m_{11}}(t) \cosh t + 16m_6 \sinh^{-6m_{12}}(t) \right\} \right] + \alpha\beta G^{\beta+1}. \quad (27)
\end{aligned}$$

From Figures 4(b), 5(b) and 6(d),  $\sigma_d$  is decreasing function of time  $t$  and it approaches to zero as time increases.

### 3.1 Cosmological Parameters

#### Jerk and Snap Parameter

Jerk parameter is used to understand the dynamics of the universe beyond mere acceleration. It measures the rate and the slowing down of cosmic expansion, the jerk provides insight into the curvature of the expansion rate itself. It is defined as

$$j = \frac{1}{H^3} \frac{\ddot{a}}{a} = \tanh^2 t. \quad (28)$$

From Figure 7, jerk  $j$  is positively increasing function of time  $t$ . Here  $j > 0$  then expansion of the universe is accelerating [27,28]. Snap parameter is obtained as

$$s = \frac{1}{H^4} \frac{\dddot{a}}{a} = \tanh^4 t, \quad (29)$$

it positively increasing function of time  $t$  implies that acceleration of the universe expansion is itself speeding up over time  $t$ . Here  $s > 0$ , it indicates that expansion of the universe is becoming more and more rapidly accelerated [28].

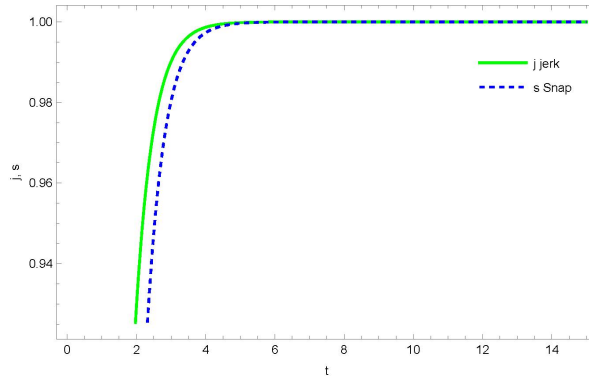


Figure 7. Graph of jerk and snap parameter vs. time  $t$ .

## 4 Case-II

we have considered the special form of deceleration parameter  $q$  proposed by Singha and Debnath [29] given by

$$q = -1 + \frac{l}{1 + a^l}, \quad (30)$$

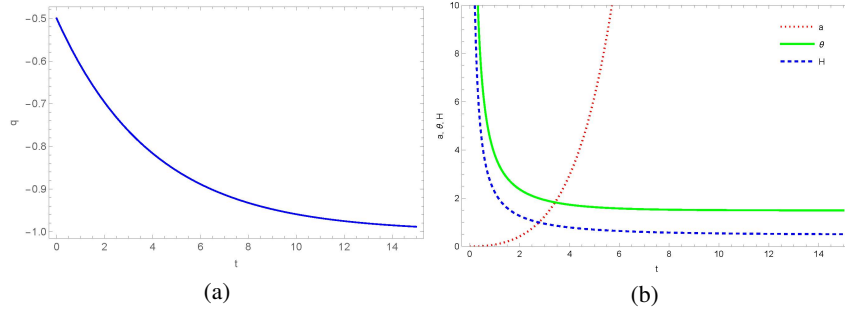


Figure 8. Graph of  $q$ ,  $a$ ,  $H$  and  $\theta$  vs. time  $t$  for  $n = 1.001$ ,  $\eta = 0.5$ ,  $l = 0.5$ .

where  $l > 0$  is constant. From Figure 8(a) universe is an accelerating phase at present time. Also the rate at which it accelerates is also increasing. Similarly from Figure 8(b) scale factor ' $a$ ' is increasing function of time  $t$

$$a(t) = (e^{\eta t} - 1)^{\frac{1}{l}} = (\tau - 1)^{\frac{1}{l}}, \quad (31)$$

where  $\tau = e^{\eta t}$  and  $\eta$  represents the integrating constant. Clearly from Figure 8(a), deceleration parameter  $q$  is decrease as time  $t$  increases. From Figure 8(b) scale factor is increasing function of time  $t$ . Here  $q < 0$  and  $a > 0$ , so universe is accelerating at the present time  $t$  [27].

Using equations (11), (30) and (31), we get metric potential  $A$  and  $B$  as

$$A = (\tau - 1)^{3nc_2} \quad \text{and} \quad B = (\tau - 1)^{3c_2}. \quad (32)$$

Cosmological parameter such as Hubble parameter  $H$ , expansion scalar  $\theta$ , shear scalar  $\sigma$  and Mean anisotropic parameter  $A_m$  are obtained as

$$H = \frac{\dot{a}}{a} = 3n\eta l c_2 \tau (\tau - 1)^{-1}, \quad (33)$$

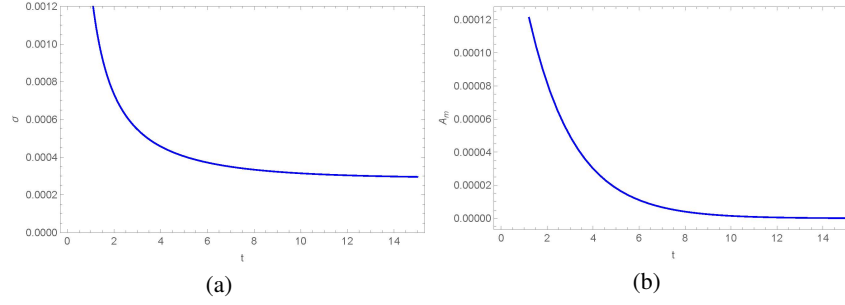
$$\theta = 3\eta l c_2 (n + 2) \tau (\tau - 1)^{-1}, \quad (34)$$

$$\sigma = \sqrt{3}\eta l c_2 (n - 1) \tau (\tau - 1)^{-1}, \quad (35)$$

$$A_m = \frac{2}{9} (n - 1) \tau^{-2}. \quad (36)$$

Clearly from Figure 8(b), Hubble parameter  $H$  and expansion scalar  $\theta$  are decreasing function of time  $t$ . Also from Figure 9(a), shear scalar  $\sigma$  is decrease as time  $t$  increases. It indicates that universe is expanding.

From Figure 9(b), mean anisotropic parameter  $A_m$  is positive and decreasing function of cosmic time  $t$ . Here  $A_m > 0$  indicates that universe started with anisotropic expansion but evolves toward isotropy.


 Figure 9. Graph of  $\sigma$  and  $A_m$  vs. time  $t$  for  $n = 1.001$ ,  $\eta = 0.5$ ,  $l = 0.5$ .

The Gauss-Bonnet invariant  $G$  is

$$G = 24nc_1 \left[ 27\eta lc_2 \tau^3 (\tau - 1)^{-3} (1 + (1 - \tau^{-1})^{-1} c_7) + k\tau (\tau - 1)^{-6c_2 - 1} (1 + (\tau - 1)^{-1} c_6) \right]. \quad (37)$$

On solving equations (8), (9), (10), and (31), after substituting value of  $A$  and  $B$ , we get

$$\begin{aligned} \rho_{\text{eff}} = & -3c_1 \tau (\tau - 1)^{-1} [n + 1 + c_3 \tau (\tau - 1)^{-1}] - c_4 \tau^2 (\tau - 1)^{-2} \\ & - 8[\eta lc_4 (\tau - 1)^{-2} (1 + \tau (\tau - 1)^{-1} c_5) + 9n\eta lc_1 c_2 \tau^2 (\tau - 1)^{-2} \\ & \times (1 + c_6 \tau (\tau - 1)^{-1})] \left[ \alpha(\beta + 1) \beta G^{\beta - 1} 24nc_1 \left\{ -81c_1 \tau^{-1} (1 - \tau^{-1})^{-4} \right. \right. \\ & \times \left[ 1 + \frac{4}{3} (1 - \tau^{-1})^{-1} c_7 \right] + k\eta l \tau^2 (\tau - 1)^{-6c_2 - 2} (-6c_2 - \tau^{-1} \\ & \left. \left. + (1 - \tau^{-1})^{-1} c_6 (-6c_2 - 2\tau^{-1}) \right\} \right] - 8c_4 \tau^2 (\tau - 1)^{-2} \\ & \times \left[ \alpha(\beta + 1) \beta (\beta - 1) G^{\beta - 2} \left\{ 24nc_1 \left\{ -81c_1 \tau^{-1} (1 - \tau^{-1})^{-4} \right. \right. \right. \\ & \times \left( 1 + \frac{4}{3} (1 - \tau^{-1})^{-1} c_7 \right) + k\eta l \tau^2 (\tau - 1)^{-6c_2 - 2} [-6c_2 - \tau^{-1} \\ & \left. \left. \left. + (1 - \tau^{-1})^{-1} c_6 (-6c_2 - 2\tau^{-1}) \right] \right\} \right\}^2 + 24nc_1 \alpha(\beta + 1) \beta G^{\beta - 1} \\ & \times \left\{ 81\eta lc_1 \tau^4 (\tau - 1)^{-5} \left( 4 \left( \tau^{-1} + \frac{4}{3} (\tau - 1)^{-1} c_7 \right) + (1 - \tau^{-1}) \right. \right. \\ & \times \left( 1 - \frac{4}{3} \tau^2 \right) (\tau - 1)^{-2} c_7 + k\eta^2 l^2 \tau (\tau - 1)^{-6c_2 - 2} [\tau (\tau - 1)^{-1} \\ & \times [-6\tau c_2 - 1 - 2(1 - \tau)^{-1} c_6 (3c_2 \tau + 1)] + [-12c_2 \tau - 1 + 2\tau (\tau - 1)^{-2} \\ & \left. \left. \left. \times c_6 (3c_2 \tau + 1) - \tau (\tau - 1)^{-1} c_6 (6c_2 \tau + 1) \right] \right\} \right\} + \alpha \beta G^{\beta + 1} \quad (38) \end{aligned}$$

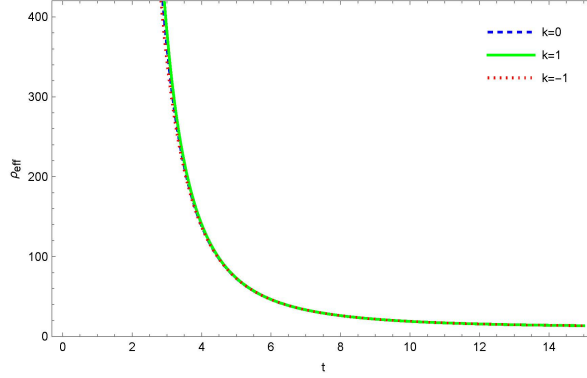


Figure 10. Graph of  $\rho_{\text{eff}}$  vs. time  $t$  for  $\eta = 0.5$ ,  $l = 0.5$ ,  $n = 1.001$ ,  $\alpha = 0.5$ ,  $\beta = 0.5$ .

From Figure 10, effective density  $\rho_{\text{eff}}$  is decreases as time  $t$  increase for  $k = 0, 1, -1$ . It approaches to zero as time  $t \rightarrow \infty$ . From Eqs. (8), (9), (11), (25) and (26) we get string tension density  $\lambda$ . Clearly from Figure 11, for  $k = 1$ , it is negatively increasing function of time  $t$  and for  $k = 0$  and  $k = -1$  it is decreasing function of time  $t$ . It approaches to zero as time  $t \rightarrow \infty$ .

Using (8), (9), (11), (17) and (37), we get

$$\begin{aligned}
\lambda = & c_9[\tau(\tau-1)^{-1} + \tau^2(\tau-1)^{-2}c_8] - k(\tau-1)^{-6c_2} + (c_{10}\tau^2(\tau-1)^{-2} \\
& \times [1 + \tau(\tau-1)^{-1}c_{12}]) \left[ \alpha(\beta+1)\beta G^{\beta-1}24nc_1 \left\{ -81c_1\tau^{-1}(1-\tau^{-1})^{-4} \right. \right. \\
& \times \left( 1 + \frac{4}{3}(1-\tau^{-1})^{-1}c_7 \right) - k\eta l\tau^2(\tau-1)^{-6c_2-2} [6c_2 + \tau^{-1} + (1-\tau^{-1})^{-1} \\
& \times c_6(6l_2 + 2\tau^{-1})] \left. \right\} - (c_{11}\tau^2(\tau-1)^{-2} + 8k(\tau-1)^{-6c_2}) \\
& \times \left[ \alpha(\beta+1)\beta(\beta-1)G^{\beta-2} \left\{ 24nc_1 \left\{ -81c_1\tau^{-1}(1-\tau^{-1})^{-4} \right. \right. \right. \\
& \times \left( 1 + \frac{4}{3}(1-\tau^{-1})^{-1}c_7 \right) k\eta l\tau^2(\tau-1)^{-6c_2-2} [-6c_2 - \tau^{-1} + (1-\tau^{-1})^{-1} \\
& \times c_6(-6c_2 - 2\tau^{-1})] \left. \right\} \left. \right\}^2 + 24nl_1\alpha(\beta+1)\beta G^{\beta-1} \left\{ -81\eta l c_1 \tau^4(\tau-1)^{-5} \right. \\
& \times \left( -4(\tau^{-1} + \frac{4}{3}(\tau-1)^{-1}c_7) - (1-\tau^{-1}) \left( 1 - \frac{4}{3}\tau^2 \right) (\tau-1)^{-2}c_7 \right) \\
& + k\eta^2 l^2 \tau(\tau-1)^{-6c_2-2} \left\{ \tau(\tau-1)^{-1} [-6\tau c_2 - 1 - 2(1-\tau)^{-1} \right. \\
& \times c_6(3c_2\tau + 1)] + [-12c_2\tau - 1 + 2\tau(\tau-1)^{-2} \\
& \times c_6(3c_2\tau + 1) - \tau(\tau-1)^{-1} c_6(6c_2\tau + 1)] \left. \right\} \left. \right\}. \tag{39}
\end{aligned}$$

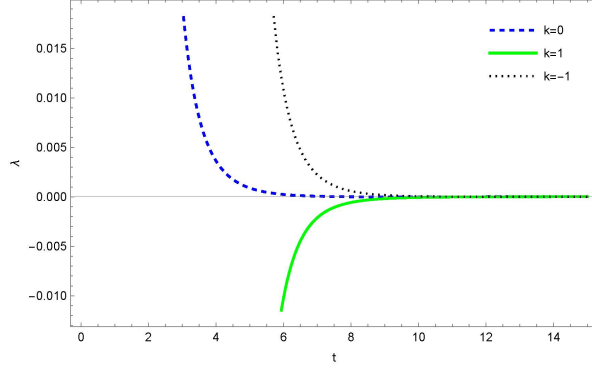


Figure 11. Graph of  $\lambda$  vs. time  $t$  for  $\eta = 0.5$ ,  $l = 0.5$ ,  $n = 1.001$ ,  $\alpha = 0.5$ ,  $\beta = 0.5$ .

From Figure 11, string tension  $\lambda$  is decreasing function of time  $t$  when  $k = 0$  and  $k = -1$ . It is negatively increasing function of time  $t$ . It approaches towards as time  $t$  increases [26].

Using equations (10), (11), (32) and (37), we get pressure

$$\begin{aligned}
 P_d = & 9c_1c_2\tau^2(\tau^2 - 1)^{-2}(2n + 1) + k(\tau - 1)^{-6c_2} + [216nc_1c_2\tau^2(\tau - 1)^2 \\
 & + 24k\eta\eta c_2(\tau - 1)^{-6c_2-1}] \left[ \alpha(\beta + 1)\beta G^{\beta-1} 24nc_1 \left\{ -81c_1\tau^{-1} \right. \right. \\
 & \times (1 - \tau^{-1})^{-4} \left( 1 + \frac{4}{3}(1 - \tau^{-1})^{-1}c_7 \right) + k\eta\tau^2(\tau - 1)^{-6c_2-2} \\
 & \left. \left. \times (-6c_2 - \tau^{-1} + (1 - \tau^{-1})^{-1}c_6(-6c_2 - 2\tau^{-1})) \right\} \right] - \alpha\beta G^{\beta+1}. \quad (40)
 \end{aligned}$$

Using equations (38) and (39), we get the energy density of the domain wall

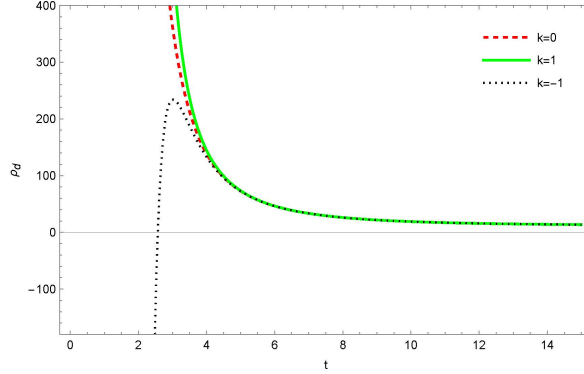
$$\begin{aligned}
 \rho_d = & -3c_1\tau(\tau - 1)^{-1}(c_{13} + \tau(\tau - 1)^{-1}c_{14}) + k(\tau - 1)^{-6c_2} \\
 & - \left\{ 72\eta c_1c_2\tau^2(\tau - 1)^{-2}(3n(1 + \tau(\tau - 1)^{-1}c_7) - c_5) \right\} \left[ \alpha(\beta + 1) \right. \\
 & \times \beta G^{\beta-1} 24nc_1 \left\{ -81c_1\tau^{-1}(1 - \tau^{-1})^{-4} \left( 1 + \frac{4}{3}(1 - \tau^{-1})^{-1}c_7 \right) \right. \\
 & \left. \left. + k\eta\tau^2(\tau - 1)^{-6c_2-2}(-6c_2 - \tau^{-1} + (1 - \tau^{-1})^{-1}c_6(-6c_2 - 2\tau^{-1})) \right\} \right] \\
 & - (72c_1c_2\tau^2(\tau - 1)^{-2} + 8k(\tau - 1)^{-6c_2}) \left[ \alpha(\beta + 1)\beta(\beta - 1)G^{\beta-2} \right. \\
 & \times \left\{ 24nc_1 \left\{ -81c_1\tau^{-1}(1 - \tau^{-1})^{-4} \left( 1 + \frac{4}{3}(1 - \tau^{-1})^{-1}c_7 \right) \right. \right. \\
 & \left. \left. + k\eta\tau^2(\tau - 1)^{-6c_2-2}(-6c_2 - \tau^{-1} + (1 - \tau^{-1})^{-1}c_6)(-6c_2 - 2\tau^{-1}) \right\} \right\}^2
 \end{aligned}$$

$$\begin{aligned}
& + (1 - \tau^{-1}) \left( 1 - \frac{4}{3} \tau^2 \right) (\tau - 1)^{-2} c_7 \Big\} + k \eta^2 l^2 \tau (\tau - 1)^{-6c_2 - 2} \\
& \times \left\{ \tau (\tau - 1)^{-1} \left( -6\tau c_2 - 1 - 2(1 - \tau)^{-1} c_6 (3c_2 \tau + 1) \right) \right. \\
& + \left( -12c_2 \tau - 1 + 2\tau (\tau - 1)^{-2} c_6 (3c_2 \tau + 1) - \tau (\tau - 1)^{-1} \right. \\
& \left. \left. \left. 6(6c_2 \tau + 1) \right) \right\} \right] + \alpha \beta G^{\beta+1}. \tag{41}
\end{aligned}$$

From Figure 12, energy density  $\rho_d$  is decreases as time  $t$  increases for  $k = 0$  and  $k = 1$ . After some fixed constant for  $k=-1$  it is decreases as time  $t$  increase. It goes to zero as time  $t \rightarrow \infty$ .

On solving equations (40) and (41), we get the equation of normal matter of domain wall

$$\begin{aligned}
\rho_m = & \frac{1}{\gamma} \left[ -3c_1 \tau (\tau - 1)^{-1} (c_{15} + \tau (\tau - 1)^{-1} c_{17}) + 2k (\tau - 1)^{-6c_2} \right. \\
& + \left\{ 72c_1 c_2 \tau^2 (\tau - 1)^{-2} (3n(1 - \eta l (1 + \tau (\tau - 1)^{-1} c_7)) + \eta l c_5) \right. \\
& + k c_{16} \tau (\tau - 1)^{-6c_2 - 1} \Big\} \left[ \alpha (\beta + 1) \beta G^{\beta - 1} 24n c_1 \left\{ -81c_1 \tau^{-1} (1 - \tau^{-1})^{-4} \right. \right. \\
& \times \left( 1 + \frac{4}{3} (1 - \tau^{-1})^{-1} c_7 \right) + k \eta l \tau^2 (\tau - 1)^{-6l_2 - 2} \\
& \times \left( -6c_2 - \tau^{-1} + (1 - \tau^{-1})^{-1} c_6 (-6c_2 - 2\tau^{-1}) \right) \Big\} \Big] \\
& - \left( 72c_1 c_2 \tau^2 (\eta l t - 1)^{-2} + 8k (\tau - 1)^{-6c_2} \right) \left[ \alpha (\beta + 1) \beta (\beta - 1) G^{\beta - 2} \right. \\
& \times \left\{ 24n c_1 \left\{ -81c_1 \tau^{-1} (1 - \tau^{-1})^{-4} \left( 1 + \frac{4}{3} (1 - \tau^{-1})^{-1} c_7 \right) \right. \right. \\
& + k \eta l \tau^2 (\tau - 1)^{-6c_2 - 2} (-6c_2 - \tau^{-1} + (1 - \tau^{-1})^{-1} c_6 (-6c_2 - 2\tau^{-1})) \Big\} \Big\}^2 \\
& + 24n c_1 \alpha (\beta + 1) \beta G^{\beta - 1} \left\{ -81\eta l c_1 \tau^4 (\tau - 1)^{-5} \left( -4 \left( \tau^{-1} + \frac{4}{3} (\tau - 1)^{-1} c_7 \right) \right. \right. \\
& - (1 - \tau^{-1}) \left( 1 - \frac{4}{3} \tau^2 \right) (\tau - 1)^{-2} c_7 \Big\} + k \eta^2 l^2 \tau (\tau - 1)^{-6c_2 - 2} \\
& \times \left[ \tau (\tau - 1)^{-1} \left( -6\tau c_2 - 1 - 2(1 - \tau)^{-1} c_6 (3c_2 \tau + 1) \right) \right. \\
& + \left( -12c_2 \tau - 1 + 2\tau (\tau - 1)^{-2} c_6 (3c_2 \tau + 1) \right. \\
& \left. \left. \left. - \tau (\tau - 1)^{-1} c_6 (6c_2 \tau + 1) \right) \right] \right] + \alpha \beta G^{\beta+1} \Big], \tag{42}
\end{aligned}$$


 Figure 12. Graph of  $\rho_d$  vs. time  $t$  for  $\eta = 0.5, l = 0.5, n = 1.001, \alpha = 0.5, \beta = 0.5$ .

where

$$\begin{aligned}
 c_1 &= \frac{\eta^2 l^2}{l(n+2)}, & c_2 &= \frac{1}{l(n+2)}, & c_3 &= (3c_2(n^2 + 1) - (n+1)), & c_4 &= 9nc_1c_2, \\
 c_5 &= (3c_2 - 1), & c_6 &= (3nc_2 - 1), & c_7 &= ((n+2)c_2 - 1), & c_8 &= (3c_2(n+2) - 1), \\
 c_9 &= 3c_1(n-1), & c_{10} &= -c_{11}\eta l, & c_{11} &= 72c_1c_2(1-n), & c_{12} &= (6c_2 - 1), \\
 c_{13} &= 3(n+1), & c_{14} &= (9c_2n - 2), & c_{15} &= 2(n+2), & c_{16} &= 24\eta lnc_2, & c_{17} &= (c_9 - 2).
 \end{aligned}$$

On solving eqs (41) and (42) we get the tension  $\sigma_d$  of domain wall

$$\begin{aligned}
 \sigma_d &= -3l_1\tau(\tau-1)^{-1} \left( c_{15} + \tau(\tau-1)^{-1}(c_1c_{13} - 2) \right) \left( 1 - \frac{1}{\gamma} \right) \\
 &\quad - 9c_1c_2\tau^2(\tau-1)^{-2} \left( 1 + \frac{2}{\gamma} \right) + k(\tau-1)^{-6c_2} \left( 1 - \frac{2}{\gamma} \right) \\
 &\quad + \left\{ 72c_1c_2\tau^2(\tau-1)^{-2} \left( (3n(1 + \tau(\tau-1)^{-1}c_7) - c_5) \right. \right. \\
 &\quad \times \left. \left( -1 + \frac{1}{\gamma} \right) \eta l - \frac{3n}{\gamma} \right) - 24kn\eta l c_2 \left( \frac{1}{\gamma} \right) \tau(\tau-1)^{-6c_2-1} \right\} \\
 &\quad \times \left[ \alpha(\beta+1)\beta G^{\beta-1} 24nc_1 \left\{ -81c_1\tau^{-1}(1-\tau^{-1})^{-4} \left( 1 + \frac{4}{3}(1-\tau^{-1})^{-1}c_7 \right) \right. \right. \\
 &\quad \left. \left. + k\eta l\tau^2(\tau-1)^{-6c_2-2} (-6c_2 - \tau^{-1} + (1-\tau^{-1})^{-1}c_6(-6c_2 - 2\tau^{-1})) \right\} \right] \\
 &\quad \times \left( 1 + \frac{4}{3}(1-\tau^{-1})^{-1}c_7 \right) + k\eta l\tau^2(\tau-1)^{-6c_2-2} \\
 &\quad \times \left( -6c_2 - \tau^{-1} - (1-\tau^{-1})^{-1}c_6(6c_2 + 2\tau^{-1}) \right) \left. \right\}^2
 \end{aligned}$$

$$\begin{aligned}
& +24nc_1\alpha(\beta+1)\beta G^{\beta-1} \left\{ -81\eta lc_1\tau^4(\tau-1)^{-5} \left( -4\tau^{-1} + \frac{16}{3}(\tau-1)^{-1}c_7 \right. \right. \\
& - (1-\tau^{-1}) \left( 1 - \frac{4}{3}\tau^2 \right) (\tau-1)^{-2} c_7 \left. \right) + k\eta^2 l^2 \tau (\tau-1)^{-6c_2-2} \\
& \times \left\{ \tau(\tau-1)^{-1} \left( -6\tau c_2 - 1 - 2(1-\tau)^{-1}c_6(3c_2\tau+1) \right) \right. \\
& + \left( -12c_2\tau - 1 + 2\tau(\tau-1)^{-2}c_6(3c_2\tau+1) - \tau(\tau-1)^{-1}c_6 \right. \\
& \left. \left. \left. (6c_2\tau+1) \right) \right\} \right\} + \left( 1 - \frac{1}{\gamma} \right) \alpha\beta G^{\beta+1}. \tag{43}
\end{aligned}$$

Clearly from Figure 13, tension  $\sigma_d$  of domain wall is decreasing function of time  $t$ . It is large near to zero and it approaches to zero as time  $t$  increases.

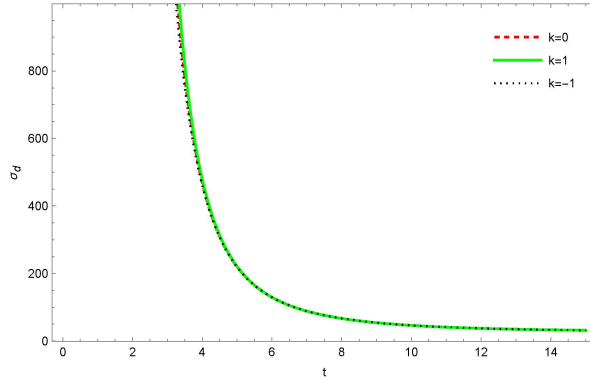


Figure 13. Graph of  $\sigma_d$  vs. time  $t$  for  $\eta = 0.5$ ,  $l = 0.5$ ,  $n = 1.001$ ,  $\alpha = 0.5$ ,  $\beta = 0.5$ .

#### 4.1 Cosmological Parameters

Jerk and snap parameter are obtained as

$$\begin{aligned}
j &= \frac{1}{\eta^3} \tau^{-3} l^2 \eta^3 (\tau-1)^{3-\frac{1}{l}} \left[ \tau(\tau-1)^{-1+\frac{1}{l}} + 3\tau^2(\tau-1)^{-2+\frac{1}{l}} \left( -1 + \frac{1}{l} \right) \right. \\
& \left. + \tau^3(\tau-1)^{-3+\frac{1}{l}} \left( -2 + \frac{1}{l} \right) \left( -1 + \frac{1}{l} \right) \right], \tag{44}
\end{aligned}$$

$$\begin{aligned}
s &= \frac{1}{\eta^4} \tau^{-4} (\tau-1)^{4-\frac{1}{l}} l^3 \eta^4 \left[ \tau(\tau-1)^{-1+\frac{1}{l}} + 7\tau^2(\tau-1)^{-2+\frac{1}{l}} \left( -1 + \frac{1}{l} \right) \right. \\
& + 6\tau^3(\tau-1)^{-3+\frac{1}{l}} \left( -2 + \frac{1}{l} \right) \left( -1 + \frac{1}{l} \right) \\
& \left. + \tau^4(\tau-1)^{-4+\frac{1}{l}} \left( -3 + \frac{1}{l} \right) \left( -2 + \frac{1}{l} \right) \left( -1 + \frac{1}{l} \right) \right]. \tag{45}
\end{aligned}$$

Clearly from Figure 14, jerk  $j$  and snap  $s$  parameters are increasing function of time  $t$ . Here  $j > 0$  and  $s > 0$ , so it indicates that expansion of the universe is accelerating [28].

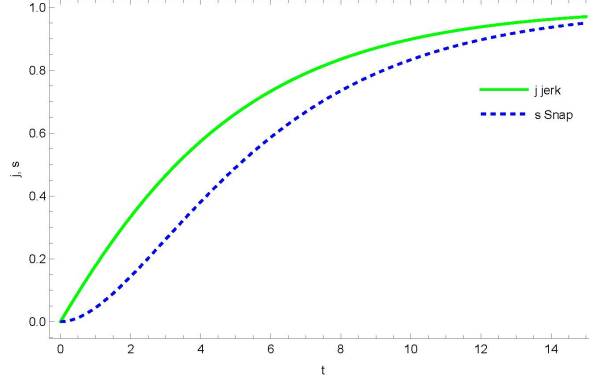


Figure 14. Graph of jerk and snap parameters vs. time  $t$  for  $\eta = 0.5$ ,  $l = 0.5$ .

## 5 Conclusion

In this paper, we have studied the behaviour of homogeneous hypersurface with cosmic string and domain wall in  $f(G)$  gravity theory of gravity. We explored the energy density  $\rho_{\text{eff}}$  and string tension density  $\lambda$  using different well-known forms of deceleration parameter  $q$ . We found that

- Case I: in this case we have used the linearly varying deceleration parameter to determine the solution to the field equation. For  $k = 0$ ,  $k = 1$ ,  $k = -1$  we found that  $H$ ,  $\theta$  and  $\sigma$  are positive and decreasing and it approaches to zero and  $t \rightarrow \infty$ . It indicates that universe is expanding with high rate of expansion. For  $k = 0$  tension  $\lambda$  is positively decreasing mode. For  $k = 0$  and  $k = -1$  it is negatively increasing mode. It approaches towards zero as time  $t$  increases. Moreover cosmological parameter jerk  $j$  and snap  $s$  are analyzed. It is found that universe is expanding with high rate of expansion. Also it is discussed mean anisotropic parameter  $A_m$ , it indicates that initially anisotropic universe evolving toward isotropy.
- Case II: In this case behaviour of  $\rho_{\text{eff}}$ ,  $\sigma_d$ ,  $\rho_d$ ,  $\theta$  and  $\sigma$  are positively decreasing functions of cosmic time  $t$  and it is similar to Case I. Tension  $\lambda$  is also positively decreasing for  $k = 0$ ,  $k = -1$ . For  $k = 1$ ,  $\lambda$  is negatively increasing function of time  $t$ . It approaches to zero as  $t$  approaches to  $\infty$ . Also, cosmological parameter jerk  $j$  and snap  $s$  are observed. It indicates that universe is expanding. Moreover mean anisotropic parameter  $A_m$  observed that universe started with anisotropic expansion but evolves towards isotropy.

## References

- [1] A. Einstein (1922) *The general theory of relativity*. Springer.
- [2] S. Capozziello, M. De Laurentis (2011) Extended theories of gravity. *Phys. Rep.* **509**(4-5) 167-321.
- [3] G. Cognola, E. Elizalde, S. Nojiri, S.D. Odintsov, S. Zerbini (2006) Dark energy in modified gauss-bonnet gravity: Late-time acceleration and the hierarchy problem. *Phys. Rev. D* **73**(8) 084007.
- [4] G.R. Bengochea, R. Ferraro (2009) Dark torsion as the cosmic speed-up. *Phys. Rev. D* **79** 124019.
- [5] T.P. Sotiriou, V. Faraoni (2010)  $f(G)$  theories of gravity. *Rev. Mod. Phys.* **82**(1) 451-497.
- [6] T. Harko (2010) Modified gravity with arbitrary coupling between matter and geometry. *Phys. Rev. D* **81** 044021.
- [7] T. Harko, F.S.N. Lobo, S. Nojiri, S. D. Odintsov (2011)  $f(R, T)$  gravity. *Phys. Rev. D* **84**(2) 024020.
- [8] S. Nojiri, S.D. Odintsov, M. Sasaki (2005) Gauss-Bonnet dark energy. *Phys. Rev. D* **71**(12) 123509.
- [9] S. Nojiri, S.D. Odintsov (2005) Modified Gauss-Bonnet theory as gravitational alternative for dark energy. *Phys. Lett. B* **631**(1-2) 1-6.
- [10] M.V. de S. Silva, M.E. Rodrigues (2018) Regular black holes in  $f(G)$  gravity. *Eur. Phys. J. C* **78** 1-18
- [11] Z. Yousaf, M. Bhatti, S. Khan, A. Malik, H.I. Alrebdi, A.-H. Abdel-Aty (2023) Stability of anisotropy pressure in self-gravitational systems in  $f(G)$  gravity. *Axioms* **12**(3) 257.
- [12] G. Abbas, D. Momeni, M. Aamir Ali, R. Myrzakulov, S. Qaisar (2015) Anisotropic compact stars in  $f(G)$  gravity. *Astrophys. Space Sci.* **357** 1-1.
- [13] A. De Felice, S. Tsujikawa (2009) Construction of cosmologically viable  $f(G)$  gravity models. *Phys. Lett. B* **675**(1) 1-8.
- [14] K. Bamba, M. Ilyas, M. Bhatti, Z. Yousaf (2017) Energy conditions in modified  $f(G)$  gravity. *Gen. Relativ. Gravit.* **49** 1-17.
- [15] A. De Felice, S. Tsujikawa (2009) Solar system constraints on  $f(G)$  gravity models. *Phys. Rev. D* **80**(6) 063516.
- [16] R. Durrer (1999) Topological defects in cosmology. *New Astron. Rev.* **43**(2-4) 111-156.
- [17] R.H. Brandenberger (1998) Topological defects and cosmology. *Pramana* **5** 191-204.
- [18] A.M. Srivastava (1999) Topological defects in cosmology. *Pramana* **53** 1069-1076.
- [19] K. Skenderis, P.K. Townsend, A. Van Proeyen (2007) Domain-wall/cosmology correspondence in ads/ds supergravity. *J. High Energy Phys.* **08** 036.
- [20] R.M. Wald (1984) *General Relativity*. University of Chicago Press.
- [21] S. Gielen, L. Marchetti, D. Oriti, *et al.* (2022) Effective cosmology from one-body operators in group field theory. *Class. Quantum Grav.* **39**(10) 105011.
- [22] A. Ashtekar, P. Singh (2023) Loop quantum cosmology: A status report. *Class. Quantum Grav.* **28**(21) 213001.

- [23] M. Sharif, H. Kausar (2011) Locally rotationally symmetric Bianchi type I cosmology in  $f(R, T)$  gravity. *Astrophys. Space Sci.* **333** 295-304.
- [24] S.D. Odintsov, V.K. Oikonomou (2015) Singular bouncing cosmology from gauss-bonnet modified gravity. *Phys. Rev. D* **92**(12) 124024.
- [25] A. Pradhan, H. Amirhashchi, B. Saha (2011) Bianchi type-i anisotropic dark energy model with constant deceleration parameter. *Int. J. Theor. Phys.* **50**, 2923-2938.
- [26] S. Hatkar, D. Tadas, S. Katore (2025) Topological defects in  $f(T)$  theory of gravity. *Eur. Phys. J. C* **85**(2) 150.
- [27] M. Visser (2004) Jerk, snap and the cosmological equation of state. *Class. Quantum Grav.* **21**(11) 2603.
- [28] S. Mallick (2023) Conharmonically flat spacetimes in frw cosmological model. *Bulg. J. Phys.* **50**(3) 311-321.
- [29] A.K. Singha, U. Debnath (2009) Accelerating universe with a special form of decelerating parameter. *Int. J. Theor. Phys.* **48** 351-356.